Case study

A comparative assessment of the physical and microstructural properties of waste garnet generated from automated and manual blasting process

Kabiru Rogo Usman[a,c], Mohd Rosli Hainin[a,b,*],
Mohd Khairul Idham Mohd Satar[a], Muhammad Naqiuddin Mohd Warid[a],
Aliyu Usman[d], Zaid Hazim Al-Saffar[a], Munder Abdullah Bilema[e]

[a] School of Civil Engineering, Universiti Teknologi Malaysia, 81310, Johor Bahru, Johor, Malaysia
[b] University Malaysia Pahang, 26600, Pekan, Pahang, Malaysia
[c] Department of Civil Engineering Technology, School of Engineering Technology, Nuhu Bamalli Polytechnic Zaria, P.M.B 1016, Zaria, Kaduna State, Nigeria
[d] Civil and Environmental Engineering Department, University Teknologi PETRONAS, Bandar Seri Iskandar, Perak, 32610, Malaysia
[e] Department of Civil Engineering, Faculty of Engineering, Benghazi University, Benghazi, Libya

ABSTRACT

Cold mix asphalt (CMA) is an eco-friendly sustainable asphalt mixture, mostly for asphalt surface treatments (ASTs). However, material compatibility and poor adhesion leading to high voids, moisture damage susceptibility, and weak early strength remain challenging. Efforts to solve this limitation is beamed towards binder improvement and modification with modifiers, adhesion promoters, or polymers. Other forms of AST mixture improvement entail supplementary cementitious reinforcing or pozzolanic agents in the form of by-products. In this study, the physio-mechanical and microstructural desirability of spent garnet for use as fine aggregate in CMA was explored. Spent garnet is a by-product of abrasive blasting, often produced in large quantities and disposed of in landfills. Often, spent garnet waste gets contaminated with toxic elements either during usage or in landfills. This study aimed to investigate the properties of Automatically (AG) and Manually generated (MG) spent garnet grades. The physio-mechanical, morphologic, and chemical parameters of spent garnet were assessed to achieve this aim. The result compared with relevant specifications on cold mixtures plus Jabatan Kerja Raya (JKR) requirement. Moreover, crystallinity and composition were studied using Fourier transform infrared (FTIR) spectroscopy, X-ray diffraction (XRD), and X-ray Fluorescence (XRF). The presence of toxic heavy metals that often contaminate spent garnet deposits in landfills was evaluated too. Results suggested that both AG and MG's high sand equivalent and least water absorption of 98 %, 89 %, and 0.14 %, 0.23 % accordingly, and can replace sand in CMA. However, MG spent garnet is not desirable for chemically sensitive materials. The AG garnet was found to be Pyrope while the MG spent garnet is largely Almandine garnet – the strongest form of garnet, including traces of other garnet forms.

© 2020 Published by Elsevier Ltd. This is an open access article under the CC BY-NC-ND license (http://creativecommons.org/licenses/by-nc-nd/4.0/).

1. Introduction

Pushing the limits in modern construction and infrastructural developments beyond conventional methods has led to an exponential rise in the use of non-renewable construction material, notably aggregates. Besides, efficient resource utilisation and conservation entails minimising non-renewable resources while recycling the enormous industrial and domestic wastes and by-products. On the other hand, significant habitat disruption of water bodies due to continuous sand mining is imminently seeking reparation. The rate of depletion of natural sand in water bodies coupled with attendant environmental consequences calls for the need to explore the use of alternative aggregates [1–4]. However, some natural aggregates are deficient in the desirable qualities required for use in pavement construction [5].

These alternative aggregates are mostly in the form of industrial by-products and wastes. Their use in cold mixtures for pavement construction and maintenance is attracting construction stakeholder's attention. Different maintenance works have varying application conditions, techniques, and materials usage. Techniques like thin asphalt overlays, crack seal [6], chip seal [7–9], mill and pave, and many others, all employ hot mix asphalt (HMA). However, cold mixtures offer the best cost-effective alternative to hot mixtures, hence gaining increased usage.

Despite gaining increased attention for its excellent resource conservation/recycling, efficient energy utilisation, and value for money, aggregate/emulsion compatibility remains a critical challenge for ensuring suitable cold mixtures for surface rehabilitation works. Hence, the need to examine the exact chemical composition, mechanical properties, and suitability of the enormous alternative aggregates. The properties of alternative aggregates in the form of waste and industrial by-products, specifically spent garnet, for use as fine aggregate replacement in pavement construction, especially cold mixtures, needs to be ascertained. To this end, the desirability for using two spent garnet grades was explored in this study in terms of physio-mechanical, chemical, and extent of the contamination.

The two grades of waste garnet are manually generated (MG) spent garnet and automatically generated (AG) spent garnet. The essence of comparing the extent of heavy metal contamination among the two categories of spent garnet is because spent garnet from manual/open sandblasting is often contaminated with foreign materials, unlike shot blasting is conducted under a strictly contained environment. Moreover, manual blasting is performed more often than the automated process due to economies of scale, thus producing an almost equivalent amount of waste, if not more than the automated method. Furthermore, the paints in most ship hulls contain heavy metals like tributyltin (TNT), and many other heavy metals, depending upon the blasted surface. TNT and other heavy metals got leached underground when used for pavement construction, contaminating soil and underground water. Groundwater contamination has been identified as a significant issue if spent garnet is used for trench backfill and soil stabilisation [10], thus, the need for investigating the safe use of spent garnet. The presence of heavy metals may mar the proper bonding and Performance of cold asphalt surface treatments (ASTs) because material compatibility is uncompromised.

For this reason, the need to ascertain the extent of toxic contamination and other mechanical properties in spent garnet for use as alternative aggregate in asphalt surface treatments for maintenance works becomes pertinent.

The use of industrial by-products as alternative aggregates for various purposes in construction has gained popularity. Several studies explored incorporating these by-products at varying percentages with recorded successes in pavement structures, concrete, and earth and soil stabilisation [11]. There is no significant research on the use of spent garnet in construction, yet, its desirable properties prompted the researcher's attention towards its use. The suitability of spent garnet as sand replacement in concrete production was studied based on its microstructural properties, and results were promising [12].

Notable among the use of spent garnet was in achieving a standard and enhanced self-compacting geopolymer concrete. Natural sand was replaced by spent garnet at percentages between 0–100% with ground granulated blast furnace slag (GGBS) as the binding medium. The study adopted a liquid/binder ratio of 0.4. The workability increases with increasing spent garnet percentage replacement. Furthermore, the durability and strengths (flexural, compressive, and splitting tensile) indicated improved performance with increasing spent garnet percentage. However, other performance measures were low, increasing the spent garnet percentage compared to control mixtures [13].

The geopolymer concrete's enhanced workability and mechanical performance are attributable to the high silica, alumina, and iron content of the added spent garnet [13]. Spent garnet also performed well in concrete subjected to an elevated temperature where the 28-day compressive strength of concrete with 20 % and 40 % yielded increases in strength of 3.8 % and 6 % respectively compared to the control [14].

Likewise, spent garnet's role in high strength alkali-activated mortars (AAMs) consisting of ground blast furnace slag (GBFS) and fly ash was promising. The mortar workability and strengths (flexural, tensile, and compressive) increase with increasing spent garnet percentage from 0 %–100 % in an increment of 25 %. An optimum percentage replacement of 25 % recorded improved durability performance measures of drying shrinkage, enhanced resistance to acid attack, and ultimate reduction in porosity and carbonation depth [15].

The only identifiable evidence in the literature on the use of spent garnet for pavement construction was the inclusion of spent garnet as fine aggregate replacement in HMA and road shoulder stabilisation. Like the previously mentioned study, 25 % garnet replacement was the optimal percentage that yielded higher stability and reduced optimum binder content than the control mixture in HMA [16]. While spent garnet up to 100 % replaced laterite for road shoulder construction proves effective [11].

Researchers conducted numerous studies on the inclusion of waste material for construction purposes [17]. These wastes are either recycled construction or demolition waste [18,19], synthetic and domestic/agricultural wastes [20,21]. Industrial by-products inclusion for construction includes ashes - bottom ash [22], fly ash [23–26], rice husk ash [27], Palm Oil Fuel Ash (POFA) [28]. Moreover, other materials are used as fillers, including stone or brick powder [29]; waste abrasives/slags – steel slag [30–35], nickel slag [36], and copper slag [37], to achieve zero or minimal impact to the environment [38]. Thus, the use of spent garnet will not be new.

MG spent garnet gets contaminated with toxic substances due to the uncontrolled blasting environment. The extent of contamination depends on the blasted surfaces, the purpose, the nature of surrounding soil depending on the initial usage, and the final deposition place [39]. Moreover, the established desirable features of garnet form the literature studied consisting of high angularity, high hardness, and density render's self as an essential alternative to natural aggregates for construction application [12,40,41].

Though efforts at minimising the leachate of heavy metal contaminants in soils were reported to be successful yet, it is an expensive and highly technical procedure requiring expertise [42].

The result of this study will be compared to JKR and ISSA-A 143 requirements for fine aggregate to be used in cold mixtures for pavement construction and rehabilitation. Additionally, it is expected to bring awareness of the safe utilisation of spent garnet in the Malaysian construction industries and the globe. It will encourage builders and engineers to use eco-friendly spent garnet-based asphalts than the conventional one made of natural river sand, create more jobs, and save the environment from further pollution.

2. Materials and methods

2.1. Garnet sand

Garnet sand is produced from quarrying garnet rocks of high to ultra-high pressure metamorphic rocks, which is regarded in some quarters as precious stones [43]. However, the argument about garnet's actual occurrence as either metamorphic, sedimentary, magmatic, detrital, or other lithological origin remained a puzzle among researchers. As such, discrimination diagrams are employed in detecting garnet's source [44]. Garnet consists of layered mineral compounds intricately joined by strong bonds. It consists of Magnesium (Mg), Ferrous iron (Fe), Ferric Iron (Fe), Aluminium (Al), Manganese (Mn), Chromium (Cr), and Calcium (Ca). These compounds' presence and concentration determine garnet's characteristic colours, which distinctly explain its type. Some of the most familiar forms of garnets as identified with their chemical formulae include Pyrope $Mg_3Al_2(SiO_4)_3$, Almandine $Fe_3Al_2(SiO_4)_3$, Spessartine $Mn_3Al_2(SiO_4)_3$, Grossularite $Ca_3Al_2(SiO_4)_3$, Andradite $Ca_3Fe_2(SiO_4)_3$, and Uvarovite $Ca_3Cr_2(SiO_4)_3$ [45] as shown in Fig. 1.

Garnet soils are produced from garnet parent rocks and are used for industrial processes requiring highly angular aggregates and exceptional hardness. Thus, garnets soils are used for abrasive blasting, especially in shipyards for cleaning ships. A large quantity of waste garnet is generated in shipyards after the blasting process and is often deposited in landfills. In Malaysia alone, Malaysia marine and heavy engineering (MMHE) imported an estimated 2000 tons of garnet soil in 2013. All the resulting waste is disposed of in landfills [12], while the garnet consumed by the AbuDhabi Marine Operation Company (ADMA-OPCO), UAE amounts to approximately 3600 tons/yr [46].

Spent garnet must be evaluated for contamination before use in construction; hence, it needs detailed microstructural evaluation. Sustainable construction has witnessed the use of unconventional aggregates like dolomite waste and steel slag.

In a related vein, use of dolomite waste as both a filler and for fine aggregate replacement in HMA recorded enhanced mechanical performance. The result of the laboratory tests has shown significant resistance to fatigue and permanent deformation for all modified mixtures [5]. Numerous other industrial by-products are used for construction purposes with safe levels of heavy metals [47].

2.2. Spent garnet samples

The AG spent garnet waste is reddish-brown while the manually blasted garnet is dark grey, Fig. 2. illustrates the striking difference between the two. The manually blasted spent garnet contains other unwanted boulders and cobbles due to the nature of the process for its generation. Further to visual inspection of the samples, further characterisation tests were conducted on a representative portion of each sample.

The waste garnet samples are subjected to mechanical, morphological, chemical, and toxicity characteristics testing. The essence of the toxicity leachate test was to ascertain the extent of contamination and, most importantly, heavy elements in the spent garnet samples. Some necessary characterisation tests form part of the Malaysian Standard requirement for AST (JKR-SPJ-2008/S4) comprising density, specific gravity, water absorption, fine aggregate angularity, and sand equivalent were conducted.

2.3. Methods and sample preparation

The MG spent garnet was sieved through a 9.50 mm test sieve to remove extraneous boulders. It was then subjected to oven-drying at 110 °C for 24 h to remove residual moisture, after which further testing was conducted. A representative

(a) Pyrope   (b) Almandine   (c) Rhodolite

(d) Uvarovite   (e) Spessartine   (f) Pink hessonite

Fig. 1. Some identified types of garnet rocks [45].
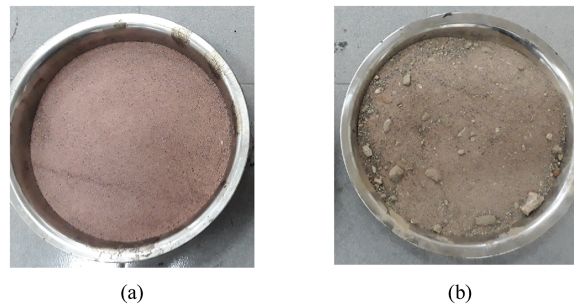

(a)   (b)

Fig. 2. Depiction of waste garnet (a) Automatically generated spent garnet (b) Manually generated spent garnet.

sample weighing 3 kg from each sample was subjected to sieve analysis by passing through progressively reducing aperture sized sieves. By so doing, the various grain sizes were graded accordingly. The gradation curves for both samples are as presented in Fig. 3.

The sample preparation for morphologic testing was achieved by further sieving via a 300 μm sieve to obtain a representative sample. The garnet size is in micrometre (μm) and powdered form, as required by XRF, FTIR, and XRD tests. These samples were subsequently subjected to the relevant testing in the laboratory. The preparation for these samples employed sieving alone to obtain the needed size for the respective tests. The preparatory sieving was done to remove unwanted material from all the samples; hence a full-scale second stage sieving was conducted as a grading test.

2.4. Physio-mechanical tests

2.4.1. Sieve analysis

A second stage sieving was done to grade the two spent garnet samples to compare with standardised mixtures. The gradation of the two garnet grades is presented in Fig. 3. The gradation of the spent garnet largely depends on the process of waste generation. Hence, due to the controlled enclosure within which automatic blasting took place, the particle sizes for the AG spent garnet indicated a single-sized or rather gap-graded type gradation. While the MG spent garnet has a range of sizes (close to uniformly graded). The AG spent garnet has grit sizes equal to or less than the new garnet's mesh size. The retained weight range starts mostly from less than 0.1 mm and some trace of fines larger than 1.0 mm. However, the MG spent garnet has traces of mixed aggregate sizes ranging from 1 mm to 9.5 mm.
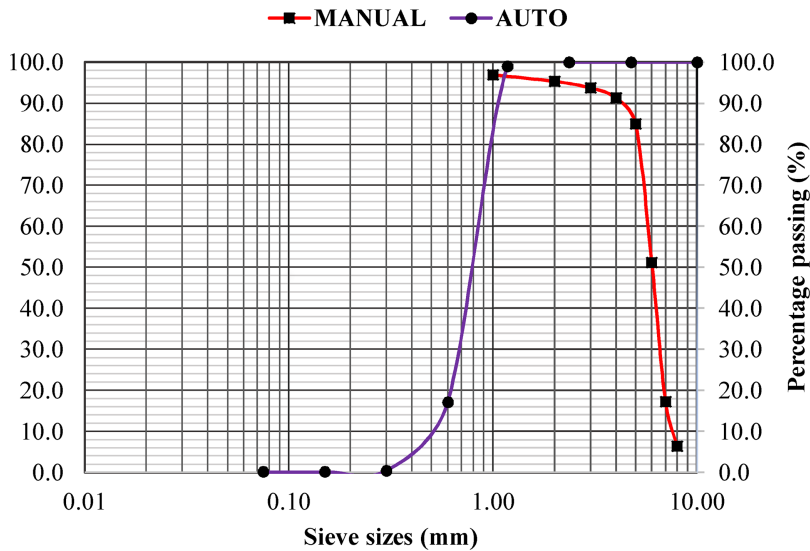
Fig. 3. Gradation of automatically and manually generated spent garnet samples.

It can be deduced from Fig. 3. that the MG garnet is a uniformly poor-graded material with a steep S-curve. Simultaneously, the AG spent garnet is a gap-graded material with a missing mid-gradation, though with the advantage of being easy to compact, with moderate permeability and void content. Unfortunately, both the two gradations did not fit within the upper and lower limits of gradations specified by the International Slurry Surfacing Association (ISSA) and JKR for aggregates for use in cold-mix emulsified asphalt slurry seals – specifically for cold mix surface treatments.

The individual gradations of AG and MG spent garnets compared to the upper and lower bounds of ISSA types II and III are presented in Figs. 4–7 accordingly. As can be seen, all the garnet samples' gradations did not fit within the two limit bounds. For this reason, a modification to the gradation is needed for full adoption in cold mixtures for ASTs.

For this reason, the spent garnet is further subjected to characterisation tests to assess its suitability in CMA, especially as a partial replacement of fine aggregate for road construction.

2.4.2. Specific gravity, density, and water absorption

Both samples' specific gravity and bulk density were tested using the gravimetric pycnometer procedure as outlined in ASTM C128 and with the air-displacement pycnometer [48]. In the gravimetric method, 6 % water by weight of the aggregate sample was added to the oven-dried and cooled sample and allowed to stand for 24 h in a closed air-tight container. A frustum cone was used to test for saturated surface dry (SSD) condition when a moulded soil sample tamped inside the mould slips after rapidly lifting it. The specific gravity and bulk density are finally computed from a weight relationship obtained by weighing the pycnometer empty, then with water, and lastly, with a combination of water and SSD soil. All the mass determination was conducted at a temperature of 25 + 5 °C as specified in ASTM standard.
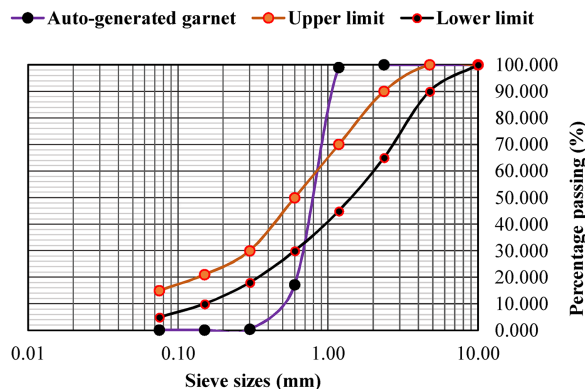

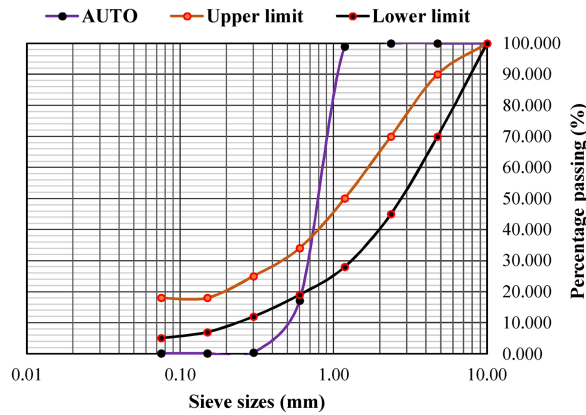**Fig. 4.** ISSA Type II gradation limits with auto-generated garnet gradation plot.

Fig. 5. ISSA Type III gradation limits with auto-generated garnet gradation plot.
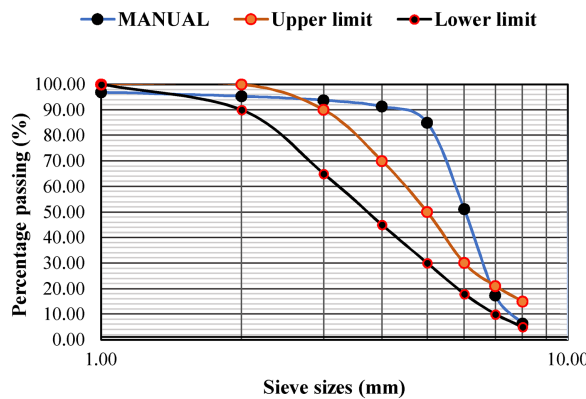

Fig. 6. ISSA Type II gradation limits with manually-generated garnet gradation plot.

The water absorption is then calculated from the relation given in Eq. (1).

$$\text{Absorption}(\%) = 100 \left[\frac{S-A}{A}\right] \tag{1}$$

'A' represents the oven-dried sample's total weight in grams, and 'S' is the weight of the saturated surface dry specimen. The specific gravity and density test were repeated using the air-displacement pycnometer by Micromeritics depicted in Fig. 8, and the result compared with that of the gravimetric method.

The density and specific gravity were analysed using an air-displacement pycnometer shown in Fig. 8. This equipment gives a more accurate and fast measurement of the specific gravity and density.

2.4.3. Fine aggregate angularity (FAA)

The test was conducted using the procedure 'A' as outlined in ASTM C1252 on a representative 190 g sample. The sample was obtained by weighing the masses retained on successive pairs of sieves from 2.36 mm, to 0.15 mm sieve. The various aggregate fractions are thoroughly mixed and placed in the glass jar, and the funnel tightened. A standard 100 mL cylinder, as in Fig. 9. was previously calibrated using distilled water at 25 °C. The weight of material emptied into the cylinder from the jar is noted and used to compute the FAA.

The Fine Aggregate Angularity (FAA) is an indirect means of measuring the texture of an aggregate. The FAA serves as an indirect measure of asphalt mixture's rutting susceptibility because angular aggregates translate to high voids in the test, and voids in asphalt mixtures translate to rutting. The FAA of aggregate is influenced by the shape, texture, size, and grading of the aggregate, as highlighted in ASTM C1252 [49]. It mainly indicates an aggregate's surface texture, which dictates workability and rutting characteristics in the final mixture of either concrete or asphalt.

The uncompacted void content is then determined from the relationship in Eq. (2).

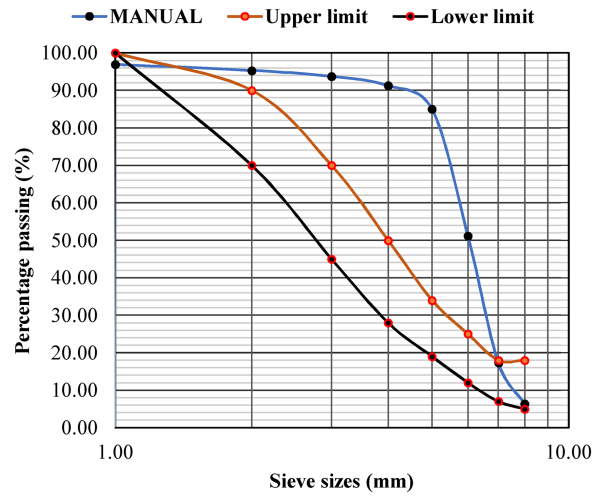$$U = V - \left[F \Big/ \frac{G]}{V \text{x}100}\right] \tag{2}$$

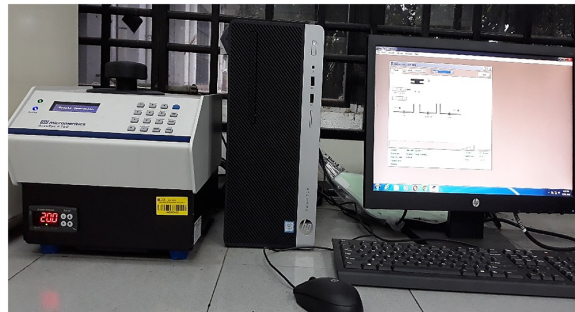**Fig. 7.** ISSA Type III gradation limits with manually-generated garnet plot.

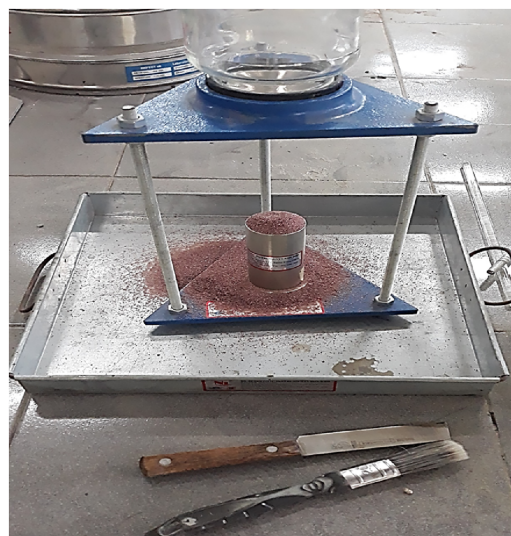**Fig. 8.** Accupyc II TEC Micromeritics air-displacement pycnometer set up.

Fig. 9. Fine Aggregate Angularity test set-up with AG spent garnet.

In which U represents the uncompacted void content of the aggregate (%), F is the net mass of combined aggregate (g), V the volume of cylindrical measure (ml), and G stands for the specific gravity of the aggregate (dry relative density).

2.4.4. Sand equivalent test

The sand equivalent is a quick site correlation test done to detect the presence or otherwise of clay or dust particles. This study adopted ASTM D 2419 [50] guideline using a representative sample from Section 2.2. The representative sample was then passed through a 4.75 mm sieve to a reduced testing sample.

The test was conducted on a saturated surface dry (SSD) portion of the reduced aggregate sample. A moisture content that forms a cast by squeezing on the palm signifies an SSD state. A duplicate set of samples were tested, and the average was reported.

In the absence of a salt stock solution for flocculating the particles in the second trial, distilled water was used instead. It was allowed to stand for one (1) week undisturbed on a flat surface after being agitated as specified [50], after which the clay and sand readings were recorded.

Clay reading was taken as the top level of the suspended material, while the sand reading is taken by inserting a standard weighted foot assembly. The reading corresponding to the white marker on the weighted foot gives the sand reading. The final sand equivalent is computed as a ratio of the sand reading to the clay reading expressed as a percentage to the nearest 0.1 %.

Higher sand equivalent test results indicate the possibility of rutting, shoving, or stripping/moisture damage in asphalt mixtures if such aggregate is used in road pavement. For this reason, morphologic testing was further employed to investigate the chemical and bonding nature of these trace particles in the spent garnet.

2.5. Microstructural and morphological tests

2.5.1. X-ray diffraction (XRD)

The samples for this test were prepared by sieving through a 0.075 mm test sieve. The samples were then placed on a flat glass plate and placed in a sample holder, as seen in Fig. 10. (c). X-Ray Diffraction (XRD) test is a fast-analytical procedure employed for the morphologic characterisation of crystalline material. Thus, the crystallinity of the spent garnets and granite samples was determined in-depth using XRD analysis. The test method works so that the crystalline atoms of the test sample cause a stream of incident X-rays from the cathode ray of the XRD machine to diffract into different specific directions.

Once the beam is split, the scatter - also called a diffraction pattern, indicates the sample's crystalline structure.

Fig. 10(a) shows a Rigaku X-ray diffractometer used for the testing, while Fig. 10(b) depicts the chamber for putting the sample holder, while Fig. 10 (c) indicates the sample holder rack. XRD is a technique used on crystalline materials for the detection of unknown crystalline lattices, phases, and positioning, which translates to structural orientation and atomic arrangements of a particular material (element); it is mostly a non-destructive test. The atomic and molecular structure of the two garnet samples is detected with their crystalline atoms, which distinctly diffract the X-rays. In turn, the diffracted rays cause a stream of incident X-rays to diffract into different specific directions.
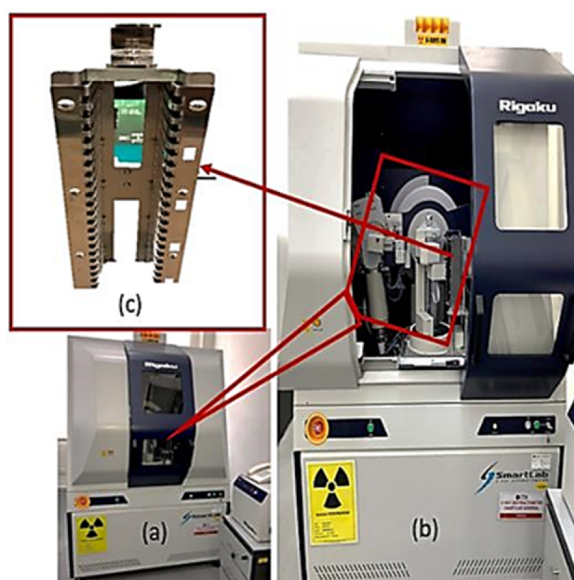

Fig. 10. (a) A Rigaku X-Ray Diffractometer, (b) XRD with sample chamber open, (c) XRD sample holder with visible sample slots or mounts.

The XRD machine produces X-rays by a cathode ray tube, filtered and reflected via the sample under testing through varying rotated angles known as 2-theta. A detector registers the reflected ray and passes it onto a computer compared with a library plot of compounds. The results were plotted as peaks of intensities against 2-theta, while the peaks compared with standard compounds and final decision on the type of compound(s) were made.

2.5.2. X-ray fluorescence (XRF)

The X-ray fluorescence spectroscopy (XRF) test was conducted on a powdered representative sample passing the 0.075 mm test sieve. The XRF test was employed to ascertain the extent of the chemical composition of the aggregate samples. A NEXCG ED XRF machine, as depicted in Fig. 11, was used.

It works by beaming an X-ray source from a triggered "unstable" isotope with adequate energy to dissociate electrons from the innermost shells of elements contained in the sample under investigation. This ray agitates the electrons with a corresponding energy release, which is peculiar to a specific element. Electrons are bonded in their respective shells by energies. Electron dissociation and release occur when the X-ray beam from the machine has higher enough energy to disembark the electron(s) from its/their orbitals.

Scientifically, the phenomenon of filling a vacant space left in an orbital by a displaced electron from emitted X-rays by another electron from lower energy orbitals is termed 'fluorescence.' The released energy is detected, received, and translated accordingly.

2.5.3. Fourier transform infrared spectroscopy (FTIR)

Fourier transforms infrared (FTIR) spectroscopy is a diagnostic procedure to detect organic and inorganic compounds. The vibration modes of the spent garnets and granite were determined using the FTIR spectrophotometer. Perking Elmer FTIR machine was used for this study, as shown in Fig. 12. The room temperature FTIR spectra in the wavenumber range of $4*10^3$ cm^{-1} to $4*10^2$ cm^{-1} are obtained.

In this study, Nitrogen gas was employed as an inert purge gas because of its abundance and low cost. With the addition of a potassium bromide (KBr) pill, a disk-shaped translucent sample was prepared and tested. The KBr pellet was degassed to perform its essence of binding together the sample particles effectively. Working at a lower frequency and higher wavelength than visible light, the principle of how FTIR works is because the light is absorbed by the varying types of bonds between

Fig. 11. NEXCG ED XRF Spectrometer.
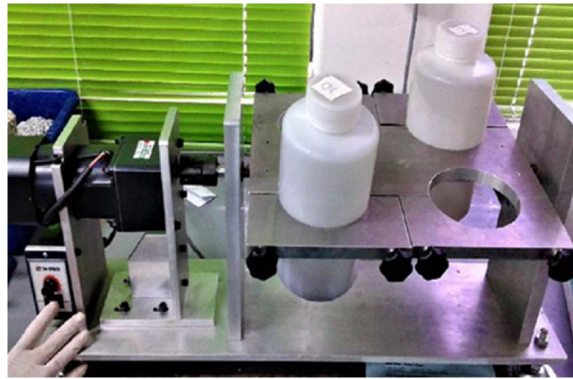

Fig. 12. An FTIR Spectrometer.

Fig. 13. Experimental set up for TCLP [12].

elements in a compound. Thus, a thin film's reflectance was feasible by a combination of potassium bromide, and the garnet sample is formed using a hydraulic press.

2.6. Chemical analysis

The essence of the toxicity leachate test was to ascertain the extent of contamination and, most importantly, toxic heavy elements in the spent garnet samples.

2.6.1. Toxicity characteristics leaching procedure test (TCLP)

The presence of possible contaminants in the form of heavy metals is evaluated using the TCLP test set shown in Fig. 13. The result is adapted from a study that used spent garnet from the same source [12] and is presented in the result section.

The possible contamination of garnet particles with other elements and mainly toxic paints from ship hulls in case of the manual blasting process needs careful assessment. To some extent, the AG spent garnet method needs evaluation in the level of contaminants as well by employing toxicity characteristics leaching procedure (TCLP) test. The test was initiated by the United States Environmental Protection Agency (US EPA) 1311 (1999). Targeted heavy metals often anticipated include Silver (Ag), Copper (Cu), Arsenic (As), Zinc (Zn), Barium (Ba), Lead (Pb), Cadmium (Cd), Selenium (Se), and Chromium (Cr). All aggregate particle sizes below 2.36 mm are considered as fine aggregates and primarily used in ASTs. Hence, it was employed in this test, and it was mixed with distilled water in the solid/liquid ratio of 1:20. Three test samples were prepared and centrifuged to facilitate agglomeration at the rate of 30 rpm for one day (Fig. 6). Filtration was used to separate the agglomerates and suspended particles using 0.45 μm sieve. The TCLP test referred to as the inductively coupled plasma mass spectrometry (ICP–MS) by the Institute of Bioproduct Development laboratory, UTM – Johor Bahru, Malaysia was conducted on the filtered leachates. The technique was employed to accurately detect the presence and extent of the heavy metal's ion contents.

3. Results and discussion

3.1. Physio-mechanical properties

The physio-mechanical characterisation test results for the two spent garnet grades, and a granite aggregate is given in Table 1. The high specific gravity of AG spent garnet of 4.08 is due to the high ferric iron oxide Fe_2O_3 content as revealed by the XRF test. The Ferric iron with an oxidation number of III (Fe^{+3}) is more massive than the ferrous iron oxide FeO, with an oxidation number of II (Fe^{+2}). Hematite is the generic name for the Ferrous oxide which is characteristically reddish. Granite aggregate has the least specific gravity, probably due to low ferric iron content. However, the reduced specific gravity of MG

Table 1
Result of the Physio-mechanical properties test on the aggregates.

Properties	Automatically Generated Spent Garnet	Manually Generated Garnet	Granite	JKR/MoRTH Specifications
Specific gravity	4.08	3.89	2.89	–
Fine aggregate angularity (FAA) (%)	58.25	45	54.13	$\geq$ 45/50
Hardness	8.0	7.5	6.0	–
Bulk Density (kg/m³)	4074	3128	1815	–
Water Absorption (%)	0.14	0.23	0.48	$\leq$ 2
Sand Equivalent (%)	98	89	96	$\geq$ 45

spent garnet of 3.89 when compared to that of AG garnet could be a result of the contamination with other soil particles or paint from the ship hull during the blasting process.

The high value of aggregate angularity - 58.25 % for the AG spent garnet and its surface texture as physically evaluated, are vital ingredients in yielding high cohesion between the binder and the coarser aggregates in an asphaltic cement. Excellent aggregate angularity enhances skid resistance in wearing courses of asphalt pavements. This grade of waste garnet could be optimally used in ASTs used for rejuvenating old asphaltic roads. The water absorption values for the three grades soil samples all fall below the limit for ASTs set by the Malaysian standard (MS 30) as highlighted in JKR. More so, the two spent garnets furnished the least absorption values of 0.14 % and 0.23 % for AG and MG spent garnets, respectively [51].

The fine aggregate angularity (FAA) of the AG garnet is higher than both the granite and MG garnet, with the latter having the least of 45 %. The low FAA of MG spent garnet could be due to contamination with silt, clay, and other particles, perhaps, unregulated grit size in the manual process. It could be due to repeated recycling of the MG spent garnet back into the blasting process. Contrary to the expectations of high-water absorption with the presence of impurities and clay particles, the MG garnet has lesser water absorption than that of granite, having 0.23 % absorption as against 0.48 % for granite.

Similarly, the sand equivalent value of the MG garnet is the least with 89 % value. Even So, all the three aggregates have passed the sand equivalent requirements for ASTs and cold mixture set by JKR, yet, the AG garnet and granite has the highest values of 98 % and 96 % respectively. Thus, both grades of waste garnets have met the sand equivalent for cold mixtures. The bulk densities are at per as well as in decreasing order from AG garnet, MG garnet, and to granite with corresponding densities of 4074 kg/m^3, 3128 kg/m^{3,} and 1815 kg/m^3 respectively.

3.2. Microstructural and morphologic tests

Assessment of the crystallinity, chemical composition, and morphological characteristics of the aggregate samples was evaluated using XRD, XRF, and FTIR tests as outlined in subsequent sections.

3.2.1. X-ray diffraction (XRD)

The result of the XRD test for AG spent garnet, MG spent garnet, and granite rock is given in Figs. 14, 15 and 16 with the combined graph in Fig. 17. The result shows that in addition to the presence of Quartz in both spent garnet samples, the AG garnet has significant traces of calcium, iron, and Zinc tecto-aluminosilicate oxide (Zn_{46} Si_{100} Al_{92} O_{384} $(ZnO)_8$ which is primarily inferred to belong to Pyrope type of garnet (($Mg_{2.23}$ $Ca_{0.38}$ $Fe_{0.45}$) ($Al_{1.8}$ $Cr_{0.11}$ $Fe_{0.04}$ $Ti_{0.01}$) Si_3 O_{12}.

The peaks in both garnet samples at 2θ range of 20–40 degrees and 50–65 degree indicate the presence of Quartz, magnesium, iron, and calcite. The highest peaks at 31.1 and 34.8 degrees corresponds to Magnesium and Aluminum components of Pyrope type garnet $Mg_3Al_2(SiO_4)_3$. While calcium, iron, and Zinc tecto-aluminosilicate oxide have progressively reducing intensities at 57.6, 75.8, and 94.2 degrees, as shown in Fig. 14. Despite the crystallinity of both grades of spent garnet, yet, MG spent garnet has peaked at 48.7, 57.4, 60.1 degrees, denoting the presence of iron and Aluminum component of almandine garnet $Fe_3Al_2(SiO_4)_3$. There is a possible presence of Rutile as evidenced in the MG spent garnet spectrum and a few other garnet types including grossular, Pyrope and andradite. Also, the peak at 92.1 degrees suggests Aluminum cobalt as inferred in the literature [12].

The XRD patterns of the manually generated (MG) garnet in Fig. 15. presents traces of many forms of garnet comprising of Rutile, andradite, Pyrope, and Almandine. The higher peaks in the MG spent garnet could be attributed to the extent of the periodicity of the atoms in the compound and their relative orbital position and a lesser extent the higher electron density and crystal orientation. The Quartz content is somewhat lower than the AG spent garnet. Traces of the possibility of being grossularite or andradite exist with the presence of iron.
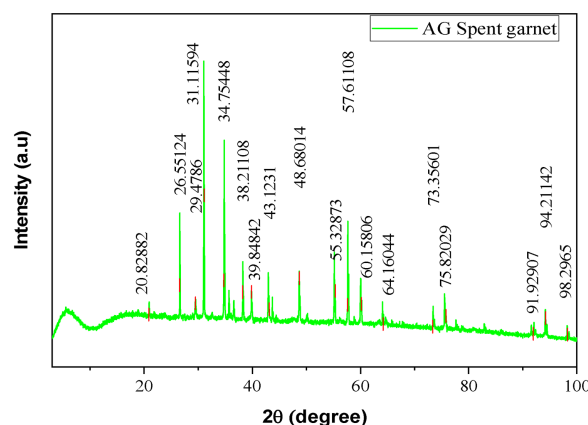

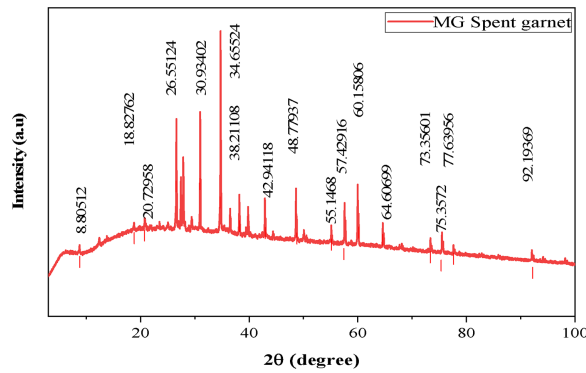**Fig. 14.** XRD result for automatically generated spent garnet.

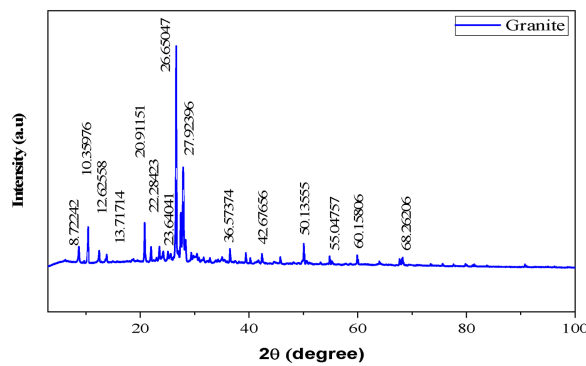**Fig. 15.** XRD result for manually generated spent garnet.

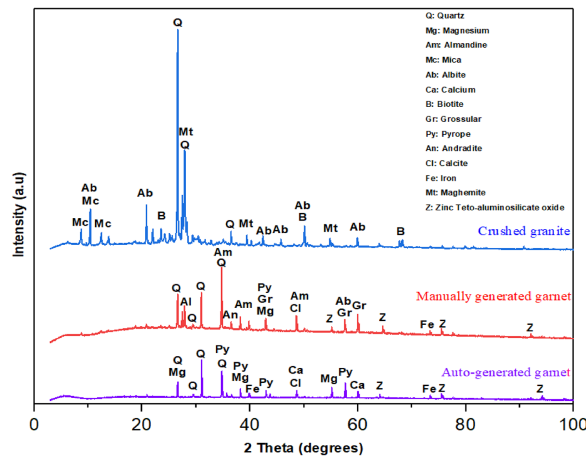**Fig. 16.** XRD result for natural crushed granite.

Fig. 17. Combined XRD result for granite, automatically, and manually generated spent garnets.

The granite peaks in Fig. 16. exhibited lesser peaks as compared to both AG and MG spent garnets, and the peaks at 26.6, 50.1, 55.0, and 60.1 degree indicates Quartz content. Albite and Mica are the peaks below 20, including peaks within 10.3, 12.6, and 13.7 degrees. It is worth noting that the Quartz high intensity in the granite spectral peak corroborates the XRF's result, which shows a high silicate content.

The combined plot for both garnet grades and granite is presented in Fig. 17. Granite is interestingly high in Quartz than both the two garnets. The high amount of Quartz content is corroborated by the XRF result in Table 2. Nonetheless, both AG and MG spent garnets have appreciable quartz contents as well, which can perform similar to what granite can offer in asphalt mixtures.

Table 2

Result of the XFR test for the two spent garnet samples and granite.

Chemical compounds	Weight percentage in automatically generated spent garnet (%)	Weight percentage in manually blasted spent garnet (%)	Weight percentage in granite (%)
Fe_2O_3	43.4	40.3	6.07
Al_2O_3	14.3	31.7	12.7
SiO_2	28.3	11.6	61.9
MgO	4.68	2.85	1.12
CaO	4.45	3.49	5.45
TiO_2	1.67	1.82	0.486
MnO	1.01	0.731	0.138
Cr_2O_3	0.106	0.032	–
ZnO	0.0484	1.04	0.0135
K_2O	0.0414	0.59	3.98
Na_2O	–	1.38	4.27
SO_3	0.0316	0.387	0.0941

3.2.2. X-ray fluorescence (XRF) test result

The result of the XRF test for the two spent garnet samples and granite is given in Table 2, which consist of a percentage number of critical compounds. The XRF technique was employed to specifically detect oxides of metals and non-metals alike in the two spent garnet grades and the granite. Table 2 indicates that the significant compound in the spent garnet is iron oxide (Fe_2O_3). The iron oxide content for AG spent garnet, MG spent garnet, and crushed granite were 43.40 %, 40.3 %, and 6.07 % respectively. Iron oxide presence in aggregates makes it heavier than normal aggregates; this explains the higher specific gravity and densities associated with the spent garnets. The alumina (Al_2O_3) content of MG spent garnet is 31.70 % which is much higher than that of AG spent garnet and granite alike, which are having 14.3 % and 12.7 % respectively. The above could be as a result of the use of a mixture of aluminium bead in the blasting operation for the manual process. Perhaps, due to mixing with cement or other alumina containing compounds in the dumpsite. The AG spent garnet's higher silicate SiO_2 content than MG spent garnet, this could be beneficial in achieving a strong calcium-silica-hydrate (C-S-H) in CMAs if cement and water are used. Undoubtedly, granite has the highest SiO_2 content of around 62 %. However, AG spent garnet has half that percentage, with 28.3 % and MG spent garnet the least with less than half the percentage of the AG spent garnet 11.6 %. Interestingly, traces of Sulfuric oxide or sulphur trioxide (SO_3) was found in all the three samples whilst sodium oxide (Na_2O) was not found in AG spent garnet; also, chromium oxide (Cr_2O_3) was absent in granite.

Traces of these heavy compounds may originate from the paints of surfaces being blasted, significantly, ship hulls which often use antifouling paints that have similar compounds. The presence of calcium and magnesium oxides (CaO & MgO) in both spent garnet samples indicated a desirable cementitious property leading to good bonding if used in asphalt and concrete as well.

Sand impurities that might have come in contact with the MG spent garnet revealed traces of Na_2, K_2O, and ZnO as depicted in Fig. 18.

3.2.3. Fourier transform infrared spectroscopy (FTIR)

The spectra overlay between the two garnet samples was similar, as such the comparison here is made between the spectra of AG garnet and that of granite. The ultimate goal is to know the extent to which garnet could replace granite
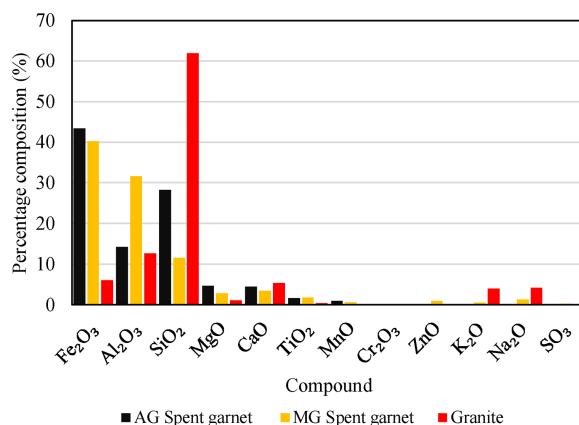

Fig. 18. Chemical composition of automatic and manually blasted garnets and crushed granite from XRF.
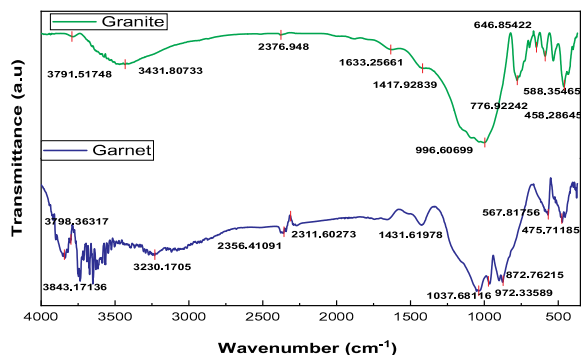
Fig. 19. Combined FTIR result for spent garnet and Granite.

aggregate in construction. The result of the FTIR test on the AG garnet and granite corroborated that of the XRD results, in Fig. 19. Moreover, the FTIR result serves as a complementing investigation to that of the XRD result [52]. The significant troughs in the graph of granite occurred in the region of organometallic compounds as depicted in Fig. 19. The first IR peaks in the range of 4000 cm^{-1} to 3500 cm^{-1} represent the O—H group, meaning the spent garnet and granite has a trace of moisture. Although there is a similar trough with that for granite, yet, the result for spent garnet Fig. 19 exhibited enormous signals in the single bond region. Meaning that compounds in that region are inferred not to be aromatic substances, whose are usually having double to triple bond combinations.

The peaks in the FTIR test result are grouped into group frequencies and fingerprint frequencies in the regions above and below 1500 cm^{-1} wavelength in a typical FTIR spectrum. While the spectra in the group frequency region detect functional groups in a molecule with high accuracy, the fingerprint regions also tell more about a molecule in a substance rather than an active group even though some functional groups are still detected in this region. Thus, the fingerprint region is a less reliable band for interpretation; hence, the absence of an IR band in the fingerprint region often present more information than its presence. Nonetheless, the IR bands 462 cm^{-1}, 558 cm^{-1}, and 772 cm^{-1} in the fingerprint region of granite are indicative of an asymmetric and symmetric active bending and stretching vibrations of Si – O bond [53].

The transmittance at 1431 cm^{-1} displayed the stretching vibration of Fe$_2$OH; this substantiates the peculiar compound of spent garnet uncovered by the XRF result. The IR spectra of spent garnet additionally revealed that the absorbance bands were due to bonding vibrations of OH and Si—O groups. The presence of these groups signifies moisture presence and the distinction of mineralogical composition.

3.3. Chemical analysis

The chemical analysis result for this study is adapted from a TCLP test of a study that used spent garnet samples from the same source.

3.3.1. Toxicity characteristic leaching procedure (TCLP)
The result of the TCLP test of MG spent garnet as adapted from [12] and [15] are presented in Table 3. Barium and zinc present the highest mass density among the other heavy toxic metals in the spent garnet sample with a value of 1.15 and

Table 3
TCLP result on manual spent garnet.

Heavy metals detected	Result (mg/l) [12]		Result (mg/L) [15]	
	Spent garnet	Regulatory limits	Spent garnet	Regulatory limits
Plumbed (Pb)	Not detected	0.05	0.009	50.0
Cadmium (Cd)	0.000445	1	0.0074	10.0
Arsenic (Ar)	0.000103	5	0.018	50.0
Barium (Ba)	1.145093	100	–	–
Nickel (Ni)	0.000159	2	0.0002	250.0
Cuprum (Cu)	0.00462	25	N.D	250.0
Zinc (Zn)	0.127609	250	N.D	250.0
Selenium (Se)	0.000757	1	–	–
Cobalt (Co)	0.00017	8	–	–
Chromium (Cr)	0.006195	5	0.0089	50.0
Beryllium (Be)	–	–	0.0001	10.0

0.13 mg/l. Generally, the concentration of all the identified toxic metals is within the United States' Environmental Protection Authority (EPA) allowable acceptable limits safe for usage.

The presence of heavy metals in spent garnet may mar its potential application in cold mix asphalt or other construction purposes due to possible contamination of underground water from its leachate. As such, the test is used to ascertain the safe application of this waste in construction. The extent of contamination of waste garnet depends on the type of application where it is used; for instance, tributyltin (TNT) is a toxic paint often used as an antifouling agent on ship hulls. The TNT gets combined with garnet wastes during the abrasive blasting process for ships painted with this chemical - TNT.

AG garnet is less prone to extraneous elements and contaminants; as such, the result of the test conducted on an MG garnet was adapted from a previous study [12]. The heavy metals checked were limited to Ag, Se, Pb, As, Ba, Cr, Zn, Cd, and Cu. The test was developed in 1976 by the resource conservation and recovery act (RCRA) of the United States (US EPA, 2015). The adapted result from Table 3 indicated that the concentrations of the highlighted heavy metals are within the regulatory safety limits set by the US environmental protection agency (EPA 2000) standards.

4. Conclusion

In this study, the comparison of the properties of spent garnets generated from automated and manual abrasive blasting was assessed as fine aggregate replacement in cold mix asphalt. The following conclusions are drawn:

1 The physio-mechanical properties of both AG and MG spent garnets as adjudged with JKR and MoRTH are satisfactory for use as cold mixtures in ASTs.
2 The AG spent garnet proved to be the best candidate for use in CMAs as compared to MG waste garnet as it yielded the least water absorption, highest FAA, sand equivalent, hardness, and density. The higher FAA of AG of 58.25 ensures more excellent interlock and bonding which helps improve rutting resistance, permanent deformation, and moisture damage resistance. While the high specific gravity of 4.08 ensures enhanced stability and durability of mixtures made with AG spent garnet aggregate.
3 The AG spent is predominantly Pyrope of origin while the MG spent garnet from almandine source coupled with a mix of andradite, grossular, and calcite.
4 It was discovered that both spent garnet grades are safe to use in cold mix asphalt and other construction purposes as the concentrations of heavy metals in them are well below the minimum acceptable EPA limits.
5 The fact that cationic emulsions could be mixed with both acid-nature and alkaline aggregates [54], the high percentage of Fe_2O_3, Al_2O_3, and SiO in both garnets, and mostly, in AG spent garnet will produce a salt which in turns is absorbed and improve aggregate-binder adhesion.
6 Hence, the outcome of the study suggested that AG spent garnet has better desirability as a candidate for use in place of fine aggregate in cold mix asphalt.

Overall, the crystallinity, high iron content, and angular nature of both grades of spent garnet provides a good characteristic for the use of the garnet waste for asphalt pavement construction. Base on the result, it is evident that the spent garnet's chemical composition is compatible with cationic type emulsions and can be used in emulsified asphalt patching mixtures.

Thus, this grade of waste garnet is recommended for use as fine aggregates suitable for cold mix asphalt construction as well as slurry AST.

Declaration of Competing Interest

The authors report no declarations of interest.

Acknowledgements

References

[1] Johnny J. Bolden, Innovative Uses of Recycled and Waste Materials in Construction Application, (2013) .
[2] C. Sing, P. Love, C. Tam, Review and exploration of river sand substitutes for concrete production in Asian countries, Adv. Civ. Eng. Build. Mater., CRC Press, 2012, pp. 115–117, doi:http://dx.doi.org/10.1201/b13165-25.
[3] M. Dan Gavriletea, Environmental impacts of sand exploitation. Analysis of sand market, Sustainable 9 (2017) 1–26, doi:http://dx.doi.org/10.3390/su9071118.
[4] W. Langer, Sustainability of Aggregates in Construction, Second edi, Elsevier Ltd., 2009, doi:http://dx.doi.org/10.1533/9781845695842.1.

[5] V. Haritonovs, J. Tihonovs, Use of unconventional aggregates in hot mix asphalt concrete, Balt. J. ROAD Bridg. Eng. 9 (2014) 276–282, doi:http://dx.doi.org/10.3846/bjrbe.2014.34.

[6] M. Jamal Khattak, M. Alrashidi, Performance of preventive maintenance treatments of flexible pavements, Int. J. Pavement Res. Technol. (2013), doi:http://dx.doi.org/10.6135/ijprt.org.tw/2013.6(3).184.

[7] M. Guirguis, A. Buss, Performance evaluation of emulsion and hot asphalt cement chip seal pavements, J. Mater. Civ. Eng. © ASCE (2017), doi:http://dx.doi.org/10.1061/(ASCE)MT.1943-5533.0002057.

[8] F. Rahman, M. Islam, H. Musty, M. Hossain, Aggregate retention in chip seal, Transp. Res. Rec. J. Transp. Res. Board (2012), doi:http://dx.doi.org/10.1533/9781845690885.4.287.

[9] J. Lee, Y. Kim, Evaluation of performance and cost-effectiveness of polymer-modified chip seals, Transp. Res. Rec. J. Transp. Res. Board (2010), doi:http://dx.doi.org/10.3141/2150-10.

[10] S. Mathews, K. Wilson, Reuse of waste cutting sand at lawrence livermore national laboratory, Air Waste Manag. Assoc. Annu. Meet. Expo., San Diego, CA, 1998.

[11] W. Noor, H. Mior, A. Mohamed, Characterization of soil mixed with Garnet Waste for road shoulder, UTM Colluquium 9 (2017) 9–14.

[12] H.L. Muttashar, N. Bin Ali, M.A. Mohd Ariffin, M.W. Hussin, Microstructures and physical properties of waste garnets as a promising construction materials, Case Stud. Constr. Mater. 8 (2018) 87–96, doi:http://dx.doi.org/10.1016/j.cscm.2017.12.001.

[13] H.L. Muttashar, M.A.M. Ariffin, M.W. Hussin, S. Bin Ishaq, Realisation of enhanced self-compacting geopolymer concrete using spent garnet as sand replacement, Mag. Concr. Res. 70 (2018) 558–569, doi:http://dx.doi.org/10.1680/jmacr.17.00212.

[14] M. Aida, A. Kadir, M.I. Khiyon, A. Rahman, M. Sam, N. Hasanah, A. Shukor, M. Najmi, M. Ali, N. Zuhan, Performance of spent garnet as a sand replacement in high-strength concrete exposed to high temperature, J. Struct. Fire Eng. 10 (2019) 468–481, doi:http://dx.doi.org/10.1108/JSFE-10-2018-0025.

[15] G.F. Huseien, A.R.M. Sam, K.W. Shah, A.M.A. Budiea, J. Mirza, Utilizing spend garnets as sand replacement in alkali-activated mortars containing fly ash and GBFS, Constr. Build. Mater. 225 (2019) 132–145, doi:http://dx.doi.org/10.1016/j.conbuildmat.2019.07.149.

[16] S.R. Aletba, N.A. Hassan, E. Aminudin, R.P. Jaya, Marshall properties of asphalt mixture containing garnet waste, J. Adv. Res. Mater. Sci. 43 (2018) 22–27. http://www.akademiabaru.com/doc/ARMSV43_N1_P22_27.pdf.

[17] A. Jamshidi, K. Kurumisawa, T. Nawa, M. Jize, G. White, Performance of pavements incorporating industrial byproducts: a state-of-the-art study, J. Clean. Prod. 164 (2017) 367–388, doi:http://dx.doi.org/10.1016/j.jclepro.2017.06.223.

[18] A. Rao, K.N. Jha, S. Misra, Use of aggregates from recycled construction and demolition waste in concrete, Resour. Conserv. Recycl. 50 (2007) 71–81, doi:http://dx.doi.org/10.1016/j.resconrec.2006.05.010.

[19] B. Gómez-Meijide, I. Pérez, Effects of the use of construction and demolition waste aggregates in cold asphalt mixtures, Constr. Build. Mater. 51 (2014) 267–277, doi:http://dx.doi.org/10.1016/j.conbuildmat.2013.10.096.

[20] P.K. Gautam, P. Kalla, A.S. Jethoo, R. Agrawal, H. Singh, Sustainable use of waste in flexible pavement: a review, Constr. Build. Mater. 180 (2018) 239–253, doi:http://dx.doi.org/10.1016/j.conbuildmat.2018.04.067.

[21] N. Su, F. Xiao, J. Wang, L. Cong, S. Amirkhanian, Productions and applications of bio-asphalts – a review, Constr. Build. Mater. 183 (2018) 578–591, doi:http://dx.doi.org/10.1016/j.conbuildmat.2018.06.118.

[22] H.K. Kim, H.K. Lee, Use of power plant bottom ash as fine and coarse aggregates in high-strength concrete, Constr. Build. Mater. 25 (2011) 1115–1122, doi:http://dx.doi.org/10.1016/j.conbuildmat.2010.06.065.

[23] N. Ali, J.S. Chan, S. Simms, R. Bushman, A.T. Bergan, Mechanistic evaluation of fly ash asphalt, J. Mater. Civ. Eng. 8 (1996) 19–25, doi:http://dx.doi.org/10.1061/(ASCE)0899-1561(1996)8:1(19).

[24] K. Sobolev, I. Flores Vivian, R. Saha, N.M. Wasiuddin, N.E. Saltibus, The effect of fly ash on the rheological properties of bituminous materials, Fuel 116 (2014) 471–477, doi:http://dx.doi.org/10.1016/j.fuel.2013.07.123.

[25] R. Mistry, T.K. Roy, Effect of using fly ash as alternative filler in hot mix asphalt, Perspect. Sci. 8 (2016) 307–309, doi:http://dx.doi.org/10.1016/j.pisc.2016.04.061.

[26] M. Ahmaruzzaman, A review on the utilization of fly ash, Prog. Energy Combust. Sci. 36 (2010) 327–363, doi:http://dx.doi.org/10.1016/j.pecs.2009.11.003.

[27] A. Behnood, M. Modiri Gharehveran, F. Gozali Asl, M. Ameri, Effects of copper slag and recycled concrete aggregate on the properties of CIR mixes with bitumen emulsion, rice husk ash, Portland cement and fly ash, Constr. Build. Mater. 96 (2015) 172–180, doi:http://dx.doi.org/10.1016/j.conbuildmat.2015.08.021.

[28] R.N.A. Raja Zulkefli, H. Yaacob, R. Putra Jaya, M.N.M. Warid, N. Hassan, M.R. Hainin, M.K. Idham, Effect of different sizes of palm oil fuel ash (POFA) towards physical properties of modified bitumen, IOP Conf. Ser. Earth Environ. Sci. 140 (2018)012108, doi:http://dx.doi.org/10.1088/1755-1315/140/1/012108.

[29] M. Arabani, S.A. Tahami, M. Taghipoor, Laboratory investigation of hot mix asphalt containing waste materials, Road Mater, Pavement Des. 18 (2017) 713–729, doi:http://dx.doi.org/10.1080/14680629.2016.1189349.

[30] P. Ahmedzade, B. Sengoz, Evaluation of steel slag coarse aggregate in hot mix asphalt concrete, J. Hazard. Mater. 165 (2009) 300–305, doi:http://dx.doi.org/10.1016/j.jhazmat.2008.09.105.

[31] S. Wu, Y. Xue, Q. Ye, Y. Chen, Utilization of steel slag as aggregates for stone mastic asphalt (SMA) mixtures, Build. Environ. 42 (2007) 2580–2585, doi:http://dx.doi.org/10.1016/j.buildenv.2006.06.008.

[32] Z. Chen, S. Wu, J. Wen, M. Zhao, M. Yi, J. Wan, Utilization of gneiss coarse aggregate and steel slag fine aggregate in asphalt mixture, Constr. Build. Mater. 93 (2015) 911–918, doi:http://dx.doi.org/10.1016/j.conbuildmat.2015.05.070.

[33] M.M.A. Aziz, M.R. Hainin, H. Yaacob, Z. Ali, F.-L. Chang, A.M. Adnan, Characterisation and utilisation of steel slag for the construction of roads and highways, Mater. Res. Innov. 18 (2014), doi:http://dx.doi.org/10.1179/1432891714Z.000000000967 S6-255-S6-259.

[34] P. Kandhal, G. Hoffman, Evaluation of steel slag fine aggregate in hot-mix asphalt mixtures, Transp. Res. Rec. 1583 (1997) 28–36, doi:http://dx.doi.org/10.3141/1583-04.

[35] M.R. Hainin, N.I.M. Yusoff, M.F. Mohammad Sabri, M.A. Abdul Aziz, M.A. Sahul Hameed, W. Farooq Reshi, Steel slag as an aggregate replacement in malaysian hot mix asphalt, ISRN Civ. Eng. 2012 (2012) 1–5, doi:http://dx.doi.org/10.5402/2012/459016.

[36] G. Wang, R. Thompson, Y. Wang, Hot-mix asphalt that contains nickel slag aggregate, Transp. Res. Rec. J. Transp. Res. Board 2208 (2011) 1–8, doi:http://dx.doi.org/10.3141/2208-01.

[37] K.S. Al-Jabri, M. Hisada, A.H. Al-Saidy, S.K. Al-Oraimi, Performance of high strength concrete made with copper slag as a fine aggregate, Constr. Build. Mater. 23 (2009) 2132–2140, doi:http://dx.doi.org/10.1016/j.conbuildmat.2008.12.013.

[38] R.J. Peploe, N. Zealand, Environmental Impact of Industrial By-products in Road Construction – a Literature Review, (2006) .

[39] N. Chillara, Abrasive Blasting Process Optimization : Enhancing Productivity, and Reducing Consumption and Solid / Hazardous Wastes, University of New Orleans, 2005.

[40] H.L. Muttashar, M.A.M. Ariffin, M.N. Hussein, M.W. Hussin, S. Bin Ishaq, Self-compacting geopolymer concrete with spend garnet as sand replacement, J. Build. Eng. 15 (2018) 85–94, doi:http://dx.doi.org/10.1016/j.jobe.2017.10.007.

[41] K.R. Usman, M.R. Hainin, M.K. Idham, M.N.M. Warid, H. Yaacob, N.A. Hassan, M. Azman, O.C. Puan, Performance evaluation of asphalt micro surfacing – a review, IOP Conf. Ser. Mater. Sci. Eng. 527 (2019)012052, doi:http://dx.doi.org/10.1088/1757-899X/527/1/012052.

[42] J. Kumpiene, A. Lagerkvist, C. Maurice, Stabilization of As, Cr, Cu, Pb and Zn in soil using amendments - a review, Waste Manag. 28 (2008) 215–225, doi:http://dx.doi.org/10.1016/j.wasman.2006.12.012.

[43] Q.X. Xia, L.G. Zhou, Different origins of garnet in high pressure to ultrahigh pressure metamorphic rocks, J. Asian Earth Sci. 145 (2017) 130–148, doi:http://dx.doi.org/10.1016/j.jseaes.2017.03.037.

[44] A. Krippner, G. Meinhold, A.C. Morton, H. Von Eynatten, Evaluation of garnet discrimination diagrams using geochemical data of garnets derived from various host rocks, Sediment. Geol. 306 (2014) 36–52, doi:http://dx.doi.org/10.1016/j.sedgeo.2014.03.004.

[45] I. Balčiunaite, A. Kleišmantas, E. Norkus, Chemical composition of rare garnets, their colours and gemmological characteristics, Chemija 26 (2015) 18–24.

[46] M.A. Maraqa, M. Al-Dhaheri, K. Saif, A. Al-Hosani, E. A-Mazrouie, Management of garnet waste generated from blasting metal structures, Arab. J. Sci. Eng. 26 (2001) 89–98.

[47] A. Jamshidi, K. Kurumisawa, T. Nawa, M. Jize, G. White, Performance of pavements incorporating industrial byproducts: a state-of-the-art study, J. Clean. Prod. 164 (2017) 367–388, doi:http://dx.doi.org/10.1016/j.jclepro.2017.06.223.

[48] ASTM C128, ASTM Standard C128 - Standard Test Method for Density, Relative Density (Specific Gravity), and Absorption, ASTM Int., 2012, pp. 1–6, doi: http://dx.doi.org/10.1520/C0128-12.1.

[49] ASTM C 1252-98, Standard test methods for uncompacted void content of fine aggregate (as influenced by particle shape, surface texture, and grading), Annu. B. Am. Soc. Test. Mater. ASTM Stand. 04 (1998) 1–5, doi:http://dx.doi.org/10.1520/C1252-06.

[50] ASTM D2419, Sand Equivalent Value of Soils and Fine Aggregate 1, ASTM, 2002, pp. 1–12, doi:http://dx.doi.org/10.1520/D2419-14.1.

[51] JKR, JKR/SPJ/2008-S4 Standard Specification for Road Works Part4 Flexible Pavement JKR Specif. Road Work. Part4 Flex. Pavement, (2008), pp. 1–187, doi:http://dx.doi.org/10.1520/A0466.

[52] S. Kaufhold, M. Hein, R. Dohrmann, K. Ufer, Quantification of the mineralogical composition of clays using FTIR spectroscopy, Vib. Spectrosc. 59 (2012) 29–39, doi:http://dx.doi.org/10.1016/j.vibspec.2011.12.012.

[53] J. Kristóf, R.L. Frost, A. Felinger, J. Mink, FTIR spectroscopic study of intercalated kaolinite, J. Mol. Struct. 410–411 (1997) 119–122, doi:http://dx.doi.org/10.1016/S0022-2860(96)09488-4.

[54] M. Ronald, F.P. Luis, Asphalt emulsions formulation: state-of-the-art and dependency of formulation on emulsions properties, Constr. Build. Mater. 123 (2016) 162–173, doi:http://dx.doi.org/10.1016/j.conbuildmat.2016.06.129.